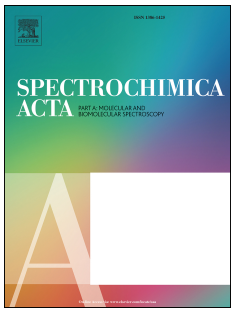

A NIR Turn-on Fluorescent Sensor For Detection of Chloride Ions in vitro and in vivo

Fengyuan Zhang, Chen Ma, Zhijuan Jiao, Shuai Mu, Yida Zhang, Xiaoyan Liu, Haixia Zhang

PII: S1386-1425(19)31119-9

DOI: https://doi.org/10.1016/j.saa.2019.117729

Reference: SAA 117729

To appear in: *Spectrochimica Acta Part A: Molecular and Biomolecular Spectroscopy*

Received Date: 11 September 2019

Revised Date: 21 October 2019

Accepted Date: 28 October 2019

Please cite this article as: F. Zhang, C. Ma, Z. Jiao, S. Mu, Y. Zhang, X. Liu, H. Zhang, A NIR Turn-on Fluorescent Sensor For Detection of Chloride Ions in vitro and in vivo, *Spectrochimica Acta Part A: Molecular and Biomolecular Spectroscopy* (2019), doi: https://doi.org/10.1016/j.saa.2019.117729.

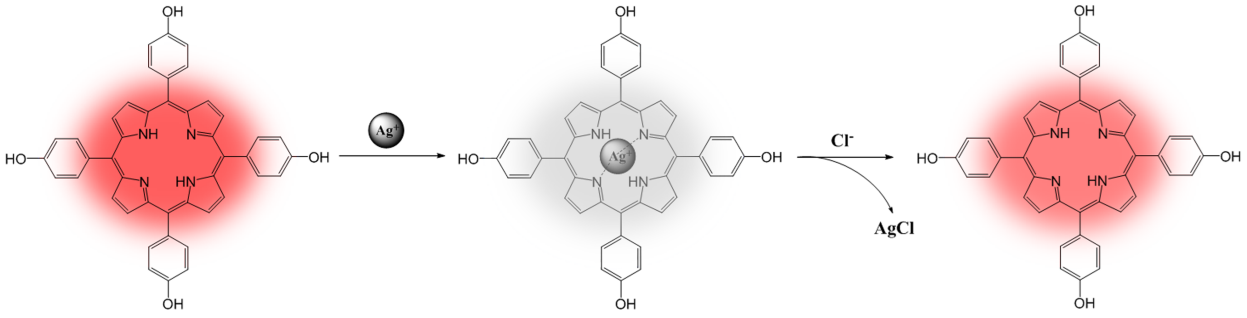

Fluorescence On **Fluorescence Silence** **Fluorescence On**

A NIR Turn-on Fluorescent Sensor For Detection of Chloride Ions in Vitro and in Vivo

Fengyuan Zhang[a,b], Chen Ma[a], Zhijuan Jiao[a], Shuai Mu[a], Yida Zhang[a], Xiaoyan Liu[a]*, Haixia Zhang[a]*

[a]State Key Laboratory of Applied Organic Chemistry and College of Chemistry and Chemical Engineering, Lanzhou University, Lanzhou 730000, China

[b]School of Basic Medical Science, Ningxia Medical University, Yinchuan 750004, China

* Corresponding author Tel: +86 931 8912058; fax: +86 931 8912058;
E-mail address: zhanghx@lzu.edu.cn

ABSTRACT: As the most abundant and significant anions in biosystem, chloride ions (Cl^-) participate in many important physiological processes. Thus, designing and synthesizing of a simple, sensitive, selective and long wavelength turn-on sensor for the detection and imaging of Cl^- in vitro and in vivo is very necessary. Herein, we have developed a simple porphyrin turn-on sensor 5, 10, 15, 20-Tetrakis (4-hydroxyphenyl) porphyrin (THPP) with near infrared emission wavelength (657 nm) for sensing chloride ions with remarkable sensitivity and selectivity. The detection of chloride ions was according to metal displacement assay (MDA) under physiological condition with a detection limit of 7.5 μM, and was applied to image Cl^- in vitro and in vivo successfully.

KEYWORDS: NIR turn-on sensor; chloride ions; in vitro; in vivo

1. Introduction

Chloride ions (Cl^-) play an indispensable role in biological field and participate various physiological processes, and distribute in almost all kinds of cells to participate many physiological processes including regulation of cell volume, control of membrane potential and keeping stability of vesicular pH value [1-4]. The homeostasis alteration of chloride levels in body fluid associates with cystic fibrosis, myotonia and startle disease [5-8]. Thus, the detection and cellular imaging of Cl^- are of great interest to chemist as well as biologist.

Owing to the simplicity, low-cost, high sensitivity, as well as in vivo and in vitro imaging, fluorescent sensors become popular to detect various ions [9-18]. The traditional anion fluorescent sensors rely on hydrogen bonding and electrostatic interactions to bind anions, which lack selectivity to distinguish different anions [19-21]. Recently, the approach based on metal-ligand coordination interaction was developed rapidly. It is superior to weak non-covalent bonding because the metal ion can selectively bind towards various anions according to their different charge and shape [22-25].

Up to now, there are extremely limited numbers of sensors available for sensing chloride ions. Among these sensors, most of them are simple quinolinium or acridinium based compounds, which are always fluorescence turn-off with limited selectivity for chloride ions [26-30]. These fluorescence turn-off sensors are limited for imaging Cl^- in vitro and in vivo because they are in silent status when encountering the abundant chloride ions in organism. The design of fluorescence turn-on sensors for chloride ions is still highly challenging. Application of the metal displacement assay to the sensor of chloride ions are hardly reported. As far as we know, only one work is that Sheri Madhu et al. reported a boron-dipyrrin-mercury (II) complex as a fluorescence turn-on sensor for chloride [31].

Here we designed and synthesized an acceptor 5, 10, 15, 20-Tetrakis (4-hydroxyphenyl) porphyrin (THPP), which coordinates with many metal cations. Among them, we selected relatively lower toxic Ag^+ to coordinate with THPP to form THPP-Ag^+, which has strong binding performance with Cl^-. Thus, a NIR fluorescence turn-on detection was obtained for Cl^-. Owing to the good spectroscopic properties, the sensor was applied to bioimaging in vitro and in vivo successfully.

2. Materials and methods

2.1. Reagents and instrumentation

4-Hydroxybenzaldehyde was purchased from Energy Chemical Technology (Shanghai, China) Co., Ltd. MTT Cell Proliferation and Cytotoxicity Assay Kit was purchased from Sangon Biotech (Shanghai, China) Co., Ltd. Pyrrole, propionic acid and ethyl acetate were refluxed at atmospheric pressure for further use. Petroleum ether and

nitrobenzene were used without additional purification. Ultrapure water was produced from the ALH-6000-U (Aquapro International Company, USA) purification system. All other chemicals were obtained from qualified reagent suppliers with analytical reagent grade.

Fluorescence spectra were recorded on a RF-5301pc fluorescence spectrometer (Shimadzu, Japan) with a xenon lamp and 1.0 cm quartz cells at the slits of 5/5 nm. High resolution mass spectra were measured using a APEX II 47e FT-ICR spectrometer with ESI or APCI positive ion mode (Bruker Daltonics, America). NMR spectra were measured using a 400 MHz instrument (JEOL, Japan). The chemical shifts (δ) were referenced to residual *d6*-DMSO (^{1}H NMR, 2.62 ppm; ^{13}C NMR, 40.76 ppm). The pH values were measured using a PHSJ-3Fdigital pH-meter (Leici, China). MTT Assay were performed using the Spark multimode microplate reader (TECAN, Switzerland). Cell imaging were performed with LSM 510 META Axiovert 200 M BP microscope (Zeiss, Germany). Animals were imaged using an IVIS Spectrum (Carestream Health, Canada).

2.2. Synthesis of THPP

Nitrobenzene (6 mL) was mixed with 8 mL of propionic acid in a 50 mL three-neck flask and refluxed for 30 min. 4-Hydroxybenzaldehyde (1.22 g, 10 mmol) was dissolved in 30 mL of propionic acid, and dropped in the above reaction mixture. At the same time, 67 mg (10 mmol) of pyrrole dissolved in 6 mL of nitrobenzene was slowly dropped into the reaction system too. The mixture was refluxed for 1.5 h, then cooled, followed by adding 10 mL of petroleum ether (40-60°C). At last, the mixture was left in the refrigerator (-20°C) overnight. The precipitate was obtained, filtered, and washed by petroleum ether. The purification was further carried out using the Soxhlet extractor with ethyl acetate as a solvent. Yield 1.102 g (65%). The pure product is in dark blue color. IR (film): ν_{max} = 3390.3, 2925.5, 1604.5, 1486.8, 1346.1, 1286.3, 1234.2, 1106.9, 846.6, 703.9 cm^{-1}; ^{1}H NMR (400 MHz, *d6*-DMSO): δ 9.91 (s, 4H), 8.83 (s, 8H), 7.95 (d, 8H), 7.16 (d, 8H); ^{13}C NMR (100 MHz, *d6*-DMSO): δ 175.7 (s), 157.9 (s), 136.1 (s), 132.5 (s), 130.3 (s), 123.8 (s), 120.6 (s), 116.2 (s), 114.5 (s); HRMS (ESI, m/z) Calcd for $C_{44}H_{30}N_4O_4$ [M + H]: 679.2340; Found: 679.2336.

2.3. Fluorescent spectra measurement

The stock solution of THPP (1.0 mM) was prepared in dimethyl sulfoxide (DMSO). The solutions containing the following ions (10.0 mM) were prepared in ultrapure water: Fe^{3+}, Al^{3+}, Zn^{2+}, Cu^{2+}, Ca^{2+}, Mg^{2+}, Ba^{2+}, Na^{+}, K^{+}, Ag^{+}, Ni^{+}, Cd^{2+}, Hg^{2+}, Pb^{2+}; CO_3^{2-}, CH_3COO^{-}, ClO_4^{-}, SO_4^{2-}, SO_3^{2-}, S^{2-}, NO_3^{-}, NO_2^{-}, F^{-}, Cl^{-}, Br^{-}, I^{-}, Pi, PPi, GSH, L-CyS. Test solutions were prepared by placing 20.0 μL of THPP (1.0 mM), 980 μL of DMSO and an appropriate aliquot of each analytic stock solution into a 2.0 mL centrifugal tube, and diluting the solution to 2.0 mL with HEPES (50.0 mM, pH = 7.4). Then the fluorescence and UV absorption spectra were recorded (RT). The fluorescence spectra were recorded with the excitation and emission wavelengths at 560/657 nm.

2.4. Real sample analysis

Human serum samples were thawed at room temperature and added to the 5 mL centrifuge tube, to which added acetonitrile, the suspension vortexed for 2 min and centrifuged under 12000 r for 5 min. The supernatant was collected and then dried with removing solvent by nitrogen-blow.

Test solutions were prepared by placing 20.0 μL of THPP (1.0 mM), 980 μL of DMSO and 20 μL of Ag^{+} (20.0 mM) into a 2.0 mL centrifugal tube and diluting the solution to 2.0 mL with 1000-fold diluted pretreated human serum. The resulting solution was shaken well at room temperature (RT) for 30 min, and then the fluorescence spectra were recorded.

2.5. In vitro and in vivo imaging

2.5.1. Cytotoxicity assay of THPP

Cytotoxic effect of THPP was measured with colorimetric methyl thiazolyl tetrazolium (MTT) assay. Hela cells (1×10^4 cells / well) were seeded in a 96-well plate in 200 μL of culture medium, then incubated for 24 h in the presence of THPP at various concentrations (0, 5, 10, 15, 20 μM). After that, MTT solution (0.5 mg/mL) was added to each well and the residual MTT solution was removed after 4 h and 100 μL of DMSO was added to each well to dissolve the formazan crystals. At last, the absorbance at 570

nm was measured with a microplate reader. The MTT assays were performed in six sets for each concentration.

2.5.2. Cell culture and confocal fluorescence imaging

HeLa cells were grown in RPMI 1640 supplemented with 10% fetal bovine serum (FBS) at 37°C and with 5% CO_2 atmosphere. Cells were plated on 14 mm glass coverslips in a 24-well plate and allowed to adhere for 12 h. Confocal luminescence imaging of cells was performed with a Zeiss Axiovert 200 M BP microscope. Excitation was carried out with a HeNe laser at 543 nm (1 mW), and emission was collected with LP 560 nm filter.

Hela cells were incubated with THPP (10 μM) for 0.5 h at 37°C, then the cells were incubated with a PBS solution of Ag^+ (200 μM) for additional 0.5 h at 37°C. After that additional Cl^- (200 μM) were added to the above system for another 0.5 h at 37°C, the imaging was recorded.

Before the imaging, the stained cells were washed three times with PBS buffer.

2.5.3. In Vivo Imaging

Kunming mice (KM, female) were obtained from Gansu University of Chinese Medicine. All animal experiments were performed abide by the guidelines issued by The Ethical Committee of Gansu University of Chinese Medicine. Kunming mice were anesthetized by intraperitoneal injection of chloral hydrate (0.1 mL, 10% in saline) and abdominal fur was removed by 8% Na_2S. The mice were imaged using an IVIS Spectrum (Carestream Health, Canada) in fluorescence mode equipped with 535 and 700 nm filters for excitation and emission respectively. Photographs were taken using a fixed exposure time.

The animal imaging experiment including four steps. (1) Kunming mice was untreated as control and took a photograph. (2) Kunming mice was given a skin-pop injection of THPP (100 μL, 100 μM) and incubated for 0.5 h, then took another photograph. (3) Kunming mice was subsequent skin-pop injection of Ag^+ (100 μL, 5 mM) at the same position and got a photograph after 0.5 h. (4) At last, Kunming mice was further subsequent additional injection of Cl^- (100 μL, 5 mM) and took a photograph after

143 0.5 h. All solutions included a mixture of HEPES buffer (50 mM, pH = 7.4) and DMSO
144 (1:1, v/v).

145 **3. Results and discussion**

146 THPP was easily synthesized via a facile one-step reaction with high yield (65%),
147 shown in Figure 1. The final product was characterized by IR, ^{1}H NMR, ^{13}C NMR and
148 HRMS, as shown in Supporting Information (Figures S1 – S4).

149 *3.1. Cl^- Analysis*

150 The fluorescence intensities for THPP under different pH values were recorded
151 (Figure 2). With the pH value from 5 to 10, the fluorescence intensities of THPP are very
152 stable. Hence, the physiological pH = 7.4 buffer was selected as experimental condition.

153 THPP can bind with metal ions easily since it has coordinating segment porphin ring
154 but no response to any anion (supporting information Fig. S5). Under low concentration
155 of metal ions (10 μM), Cu^{2+} is the most sensitive ion to coordinate with THPP (Fig. S6).
156 Thus, THPP could detect trace Cu^{2+} with preferable sensitivity (supporting information
157 Fig. S7-S9).

158 Nevertheless, with the addition of high concentration of various metal ions (500
159 μM), the fluorescence of THPP can be quenched with various other ions including Ag^{+},
160 Pb^{2+}, Cd^{2+} and Hg^{2+} (Figure 3). Owing to the high toxicity, Pb^{2+}, Cd^{2+} and Hg^{2+} were
161 unsuitable to employed in any analysis procedure. Thinking about the less toxicity and
162 stronger binding ability to Cl^-, Ag^{+} was selected for the Cl^- detection in biological
163 samples. The association constant of THPP with Ag^{+} was determined to be 0.5×10^4 M^{-1}
164 (Supporting Information Figure S10). In order to select the optimal test condition,
165 different concentrations of Ag^{+} (50–500 μM) were added into THPP to quench the
166 fluorescence intensity respectively. From figure 4, the fluorescence intensity was
167 unchanged when the concentration of Ag^{+} below 100 μM. While, the concentration of
168 Ag^{+} were raised up to 200 μM, the fluorescence intensity was quenched obviously. The
169 fluorescence was quenched almost completely till the concentration of Ag^{+} beyond 300

μM. Thus, the optimal concentration of Ag^+ is 300 μM. So we selected the THPP-Ag^+ (10 μM - 300 μM) to quantitative analysis of Cl^-.

The selectivity and coexisting ion interference experiments of THPP-Ag^+ towards various anions, including CO_3^{2-}, CH_3COO^-, ClO_4^-, SO_4^{2-}, SO_3^{2-}, NO_3^-, NO_2^-, F^-, Cl^-, Br^-, I^-, Pi, PPi and S^{2-} were carried out in H_2O/DMSO solution (1:1, v/v, 50.0 mM HEPES, pH = 7.4). As shown in Figure 5, other anions caused no changes in the fluorescence intensity except Br^- and S^{2-}. However, bromine concentration about 17.9~63 μM which are much lower than the concentration of Cl^- (100 mM) in plasma or serum [26, 32]. So its interference can be ignored. Although free S^{2-} is hard to find in body fluid, but consideration of many amino acid containing mercapto groups in vivo, so we have investigate the selectivity and coexisting interference of THPP-Ag^+ towards GSH and L-Cys which are the most abundant amino acid containing mercapto groups (Fig.5). We found, although free S^{2-} can recover the fluorescence intensity of THPP-Ag^+, but GSH and L-Cys have a bit of response with THPP-Ag^+ and there is no interference to detection of Cl^-. The selectivity of THPP-Ag^+ towards chloride ions is superior to the most of other Cl^- sensors, which is listed in the Table 1. Successive addition of Cl^- to the above system, fluorescence intensity can be recovered gradually (Figure 6A). The detection limit of Cl^- was calculated to be 7.5 μM (Figure 6B) which is superior to the most of Cl^--sensors. Table 1 gave the comparison between THPP-Ag^+ and the reported Cl^- fluorescence sensors.

Table 1. Comparison of sensor THPP-Ag^+ with reported fluorescence Cl^- sensors

Cl^- Sensors	Emission Wavelength /nm	Linear range /μM	LOD[a] /μM	pH value	Selectivity	Reference

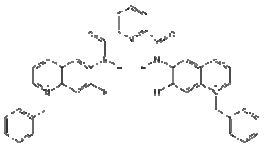	460 Emission off	—	33	5.0	Cl^- ~I^- > Br^- >> F^-	[33]
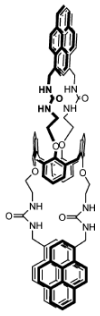	452 Emission Off	—	8	—	Only Cl^-	[34]
Zwitterionic receptor 1 Dicationic receptor 2	1. 510 Emission On 2. 510 Emission On	100 - 3000 50 - 3000	300 150	7.0 7.0	Cl^- > AcO^- > HCO_3^- > $H_3P_2O_7^-$ Cl^- > AcO^- > $H_3P_2O_7^-$ > SO_4^{2-} > $H_2PO_4^-$ > HCO_3^- > NO_3^- > F^-	[35]
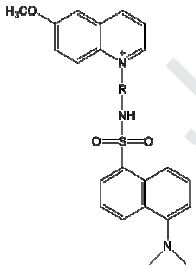	Ratiometric Fluorescence F_{560nm}/F_{440nm}	0-10^5	180	4.5	—	[36]

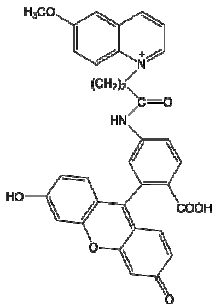	Ratiometric Fluorescence F_{519nm}/F_{436nm}	—	480	7.4	Br^-, I^-	[37]
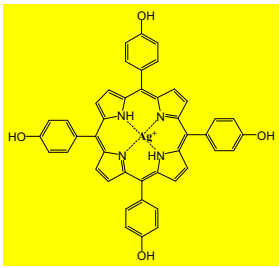	657 Emission On	20 -140	7.5	7.4	$Cl^- > Br^-$	This work

[a]Limit of detection

— Not list in paper

3.2. Application

3.2.1. Real Sample Analysis

Table 2 The detection of Cl^- in serum sample

Sample	Method	[Cl^-] detected (C/mM)
Human serum	THPP-Ag^+	120.8 ± 1.8
	Precipitation titration	113.3 ± 0.4

First, the proposed method was applied to the analysis of chloride ions in human serum samples. The chloride ions in human serum was evaluated by this method and the standard precipitation titration method. Essentially identical results were obtained by these two methods (Table 2), indicating that the proposed method could be used for Cl^- detection in serum samples.

3.2.2. Cell Imaging

Owing to the stable pH value and good spectroscopic properties, THPP was applied

to confocal fluorescence imaging in Hela cells. MTT assay showed (Figure 7) that THPP had no significant cytotoxicity (cell viability ≥ 80%) when Hela cells was treated with THPP (<15 μM) for 24 h. Thus, 10 μM of THPP is selected for cell imaging.

The cell imaging was performed and shown in Figure 8. Hela cells were incubated with THPP (10 μM) at 37°C for 0.5 h and showed strong red fluorescence (Figure 8B). After addition of Ag^+ (200 μM) for another 0.5 h, the fluorescence was quenched a lot but can not be quenched completely (Figure 8C). This is due to the presence of chloride ions in the cell. At last, Cl^- (200 μM) recovered the fluorescence some extent (Figure 8D). The cell imaging experiment demonstrated that sensor THPP can permeate through the cytomembrane and detect chloride ions under cellular environment.

3.2.3. In Vivo Imaging

THPP are propitious to apply in vivo imaging that can eliminate the interference from background auto-fluorescence and minimize the optical damage to living body. As shown in the Figure 9. with skin-pop injection of the probe THPP, regional fluorescence enhanced (Figure 9B). Ag^+ quenched the fluorescence (Figure 9C) and then Cl^- recover the fluorescence (Figure 9D). It was revealed that THPP could image Cl^- in living mice.

4. Conclusions

In summary, we have developed a novel NIR fluorescence turn-on sensor THPP for the sensitive detection of chloride ions under physiological condition by a simple MDA method with preferable sensitivity and selectivity. At last, depend on the remarkable spectroscopic properties, the sensor THPP was applied to image Cl^- in vitro and in vivo successfully.

Acknowledgements

This work was financially supported by National Natural Science Foundation of China (No.21575055) and Fundamental Research Funds for the Central Universities (lzujbky-2017-k09).

Supporting Information

Details of additional figures, tables, IR, NMR and HRMS spectra in the text.

Notes

The authors declare no competing financial interest.

References

[1] V. Faundez, H.C. Hartzell, Intracellular Chloride Channels: Determinants of Function in the Endosomal Pathway, Sci Signaling, 2004(233):re8.

[2] T.J. Jentsch, V. Stein, F. Weinreich, A.A. Zdebik, Molecular Structure and Physiological Function of Chloride Channels, Physiol Rev., 82 (2002) 503-568.

[3] H. Wolosker, D.O. de Souza, L. de Meis, Regulation of Glutamate Transport into Synaptic Vesicles by Chloride and Proton Gradient, J. Biol. Chem., 271 (1996) 11726-11731.

[4] E. Maeno, Y. Ishizaki, T. Kanaseki, A. Hazama, Y. Okada, Normotonic cell shrinkage because of disordered volume regulation is an early prerequisite to apoptosis, Proc Natl Acad Sci U S A., 97 (2000) 9487.

[5] R. Planells-Cases, T.J. Jentsch, Chloride channelopathies, BBA-Mol Basis Dis., 1792 (2009) 173-189.

[6] A. Graefe, S.E. Stanca, S. Nietzsche, L. Kubicova, R. Beckert, C. Biskup, G.J. Mohr, Development and Critical Evaluation of Fluorescent Chloride Nanosensors, Anal. Chem., 80 (2008) 6526-6531.

[7] T.J. Jentsch, C.A. Hübner, J.C. Fuhrmann, Ion channels: Function unravelled by dysfunction, Nat Cell Biol., 6 (2004) 1039.

[8] W.J. Warwick, N.N. Huang, W.W. Waring, A.G. Cherian, I. Brown, E. Stejskal-Lorenz, W.H. Yeung, G. Duhon, J.G. Hill, D. Strominger, Evaluation of a cystic fibrosis screening system incorporating a miniature sweat stimulator and disposable chloride sensor, Clin. Chem., 32 (1986) 850.

[9] S. Zhang, Q. Wang, X. Liu, J. Zhang, X.-F. Yang, Z. Li, H. Li, Sensitive and Selective Fluorescent Probe for Selenol in Living Cells Designed via a pKa Shift Strategy, Anal. Chem., 90 (2018) 4119-4125.

[10] V. Susini, A. Ienco, V. Lucia Rossi, A. Paolicchi, A. Sanesi, Fluorescence enhancement aided by metal ion displacement, Biosens. Bioelectron., 80 (2016) 237-242.

[11] G. Wang, H. Qi, X.-F. Yang, A ratiometric fluorescent probe for bisulphite anion, employing intramolecular charge transfer, Luminescence, 28 (2012) 97-101.

[12] P. Marimuthu, A. Ramu, A ratiometric fluorescence chemosensor for Mg2+ ion and its live cell imaging, Sens Actuators B: Chem., 266 (2018) 384-391.

[13] X.-j. Zhao, Y.-r. Jiang, Y.-x. Chen, B.-q. Yang, Y.-t. Li, Z.-h. Liu, C. Liu, A new “off-on” NIR fluorescence probe for determination and bio-imaging of mitochondrial hypochlorite in living cells and zebrafish, Spectrochim. Acta A, 219 (2019) 509-516.

[14] M. Faraz, A. Abbasi, F.K. Naqvi, N. Khare, R. Prasad, I. Barman, R. Pandey, Polyindole/cadmium sulphide nanocomposite based turn-on, multi-ion fluorescence sensor for detection of Cr3+, Fe3+ and Sn2+ ions, Sens Actuators B: Chem., 269 (2018) 195-202.

[15] R. Zeng, Q. Gao, F. Cheng, Y. Yang, P. Zhang, S. Chen, H. Yang, J. Chen, Y. Long, A near-infrared fluorescent sensor with large Stokes shift for rapid and highly selective detection of thiophenols in water samples and living cells, Anal Bioanal Chem., 410 (2018) 2001-2009.

[16] H. Li, X. Wang, Z. Cai, L. Lu, J. Tao, B. Sun, Y. Yang, Q. Xu, Z. Yu, P. Zhao, Ratiometric fluorescent sensing of copper ion based on chromaticity change strategy, Anal Bioanal Chem., 409 (2017) 6655-6662.

[17] Y. Jin, M. Lv, Y. Tao, S. Xu, J. He, J. Zhang, W. Zhao, A water-soluble BODIPY-based fluorescent probe for rapid and selective detection of hypochlorous acid in living cells, Spectrochim. Acta A, 219 (2019) 569-575.

[18] H. Chen, X. Gong, X. Liu, Z. Li, J. Zhang, X.-F. Yang, A nitroso-based fluorogenic probe for rapid detection of hydrogen sulfide in living cells, Sens Actuators B: Chem., 281 (2019) 542-548.

[19] P. Sokkalingam, D.S. Kim, H. Hwang, J.L. Sessler, C.-H. Lee, A dicationic calix[4]pyrrole derivative and its use for the selective recognition and displacement-based sensing of pyrophosphate, Chem Sci., 3 (2012) 1819-1824.

[20] C. Caltagirone, C. Bazzicalupi, F. Isaia, M.E. Light, V. Lippolis, R. Montis, S. Murgia, M. Olivari, G. Picci, A new family of bis-ureidic receptors for pyrophosphate optical sensing, Org Biomol Chem., 11 (2013) 2445-2451.

[21] Z. Xu, J.-Y. Choi, J.-Y. Yoon, Fluorescence Sensing of Dihydrogen Phosphate and Pyrophosphate using Imidazolium Anthracene Derivatives, Bull. Korean Chem. Soc., 32 (2011) 1371-1374.

[22] H.T. Ngo, X. Liu, K.A. Jolliffe, Anion recognition and sensing with Zn(ii)-dipicolylamine complexes, Chem. Soc. Rev., 41 (2012) 4928-4965.

[23] J.F. Zhang, S. Kim, J.H. Han, S.-J. Lee, T. Pradhan, Q.Y. Cao, S.J. Lee, C. Kang, J.S. Kim, Pyrophosphate-Selective Fluorescent Chemosensor Based on 1,8-Naphthalimide–DPA–Zn(II) Complex and Its Application for Cell Imaging, Org. Lett., 13 (2011) 5294-5297.

[24] J.-R. Lin, C.-J. Chu, P. Venkatesan, S.-P. Wu, Zinc(II) and pyrophosphate selective fluorescence probe and its application to living cell imaging, Sens Actuators B: Chem., 207 (2015) 563-570.

[25] S.-Y. Jiao, K. Li, X. Wang, Z. Huang, L. Pu, X.-Q. Yu, Making pyrophosphate visible: the first precipitable and real-time fluorescent sensor for pyrophosphate in aqueous solution, Analyst, 140 (2015) 174-181.

[26] C.D. Geddes, K. Apperson, J. Karolin, D.J.S. Birch, Chloride-Sensitive Fluorescent Indicators, Anal. Biochem., 293 (2001) 60-66.

[27] S. Jayaraman, L. Teitler, B. Skalski, A.S. Verkman, Long-wavelength iodide-sensitive fluorescent indicators for measurement of functional CFTR expression in cells, Am J Physiol Cell Physiol, 277 (1999) C1008-C1018.

[28] A.S. Verkman, Development and biological applications of chloride-sensitive fluorescent indicators, Am J Physiol Cell Physiol, 259 (1990) C375-C388.

[29] J. Biwersi, B. Tulk, A.S. Verkman, Long-Wavelength Chloride-Sensitive Fluorescent Indicators, Anal. Biochem., 219 (1994) 139-143.

[30] B.A. McNally, A.V. Koulov, B.D. Smith, J.-B. Joos, A.P. Davis, A fluorescent assay for chloride transport; identification of a synthetic anionophore with improved activity, Chem. Commun., (2005) 1087-1089.

[31] S. Madhu, R. Kalaiyarasi, S.K. Basu, S. Jadhav, M. Ravikanth, A boron-dipyrrin-mercury(ii) complex as a fluorescence turn-on sensor for chloride and applications towards logic gates, J. Mater. Chem. C., 2 (2014) 2534-2544.

[32] J. Versieck, R. Cornelis, Normal levels of trace elements in human blood plasma or serum, Anal. Chim. Acta, 116 (1980) 217-254.

[33] I.J. Bazany-Rodríguez, D. Martínez-Otero, J. Barroso-Flores, A.K. Yatsimirsky, A. Dorazco-González, Sensitive water-soluble fluorescent chemosensor for chloride based on a bisquinolinium pyridine-dicarboxamide compound, Sens Actuators B: Chem., 221 (2015) 1348-1355.

[34] B. Schazmann, N. Alhashimy, D. Diamond, Chloride Selective Calix[4]arene Optical Sensor Combining Urea Functionality with Pyrene Excimer Transduction, J. Am. Chem. Soc., 128 (2006) 8607-8614.

[35] T. Riis-Johannessen, K. Schenk, K. Severin, Turn-Off-and-On: Chemosensing Ensembles for Sensing Chloride in Water by Fluorescence Spectroscopy, Inorg. Chem., 49 (2010) 9546-9553.

[36] P. Li, S. Zhang, N. Fan, H. Xiao, W. Zhang, W. Zhang, H. Wang, B. Tang, Quantitative Fluorescence Ratio Imaging of Intralysosomal Chloride Ions with Single Excitation/Dual Maximum Emission, Chem. Eur. J., 20 (2014) 11760-11767.

[37] P. Li, T. Xie, N. Fan, K. Li, B. Tang, Ratiometric fluorescence imaging for distinguishing chloride concentration between normal and ischemic ventricular myocytes, Chem. Commun., 48 (2012) 2077-2079.

Captions

Fig. 1 Synthesis of THPP

Fig. 2 Fluorescence intensity of THPP (10 μM) under the different pH values (5 - 10). Data points represent the mean of three independent experiments (± SD).

Fig.3 Fluorescence response of THPP (10.0 μM) in the presence of 50.0 equiv. of different cations (Fe^{3+}, Al^{3+}, Zn^{2+}, Cu^{2+}, Ca^{2+}, Mg^{2+}, Ba^{2+}, Na^{+}, K^{+}, Ag^{+}, Ni^{+}, Cd^{2+}, Hg^{2+}, Pb^{2+}). H_2O/DMSO solution (1:1, v/v, 50.0 mM HEPES, pH = 7.4) (λ_{ex} = 560 nm, λ_{em} = 657 nm). Data points represent the mean of three independent experiments (± SD).

Fig.4 Fluorescence response of THPP (10.0 μM) in the presence of different concentrations of Ag^{+} (0, 50, 100, 200, 300, 400, 500 μM). H_2O/DMSO solution (1:1, v/v, 50.0 mM HEPES, pH = 7.4) (λ_{ex} = 560 nm, λ_{em} = 657 nm). Data points represent the mean of three independent experiments (± SD).

Fig.5 Fluorescence response of THPP-Ag^{+} in the presence of different anions (CO_3^{2-}, CH_3COO^{-}, ClO_4^{-}, SO_4^{2-}, SO_3^{2-}, S^{2-}, NO_3^{-}, NO_2^{-}, F^{-}, Cl^{-}, Br^{-}, I^{-}, PPi, Pi, GSH, L-CyS) (black bars) and in the presence of Cl^{-} plus other competitive species coexisting (red bars). H_2O/DMSO solution (1:1, v/v, 50.0 mM HEPES, pH = 7.4) (λ_{ex} = 560 nm, λ_{em} = 657 nm). Data points represent the mean of three independent experiments (± SD).

Fig. 6 (A) Fluorescence titration of THPP-Ag^{+} upon addition of 0-500 μM of Cl^{-}. (B) Linear response of the emission intensity changes of THPP-Ag^{+} with the concentration of Cl^{-}. H_2O/DMSO solution (1:1, v/v, 50.0 mM HEPES, pH = 7.4). (λ_{ex} = 560 nm, λ_{em} = 657 nm). Data points represent the mean of three independent experiments (± SD).

Fig.7 Effect of THPP on the viability of Hela cells after incubation of 24 h.

Fig. 8 Confocal fluorescence images of Hela cells. (A) Untreated control cells. (B) Cells incubated with THPP (10.0 μM) for 0.5 h. (C) Cells incubated with THPP (10.0 μM) for 0.5 h, then Ag^+ (200.0 μM) for another 0.5 h. (D) Cells incubated with THPP (10.0 μM) for 0.5 h, Ag^+ (200.0 μM) for 0.5 h, then Cl^- (200.0 μM) for another 0.5 h. Bright field (1), fluorescence (2) and overlap field (3). Scale bars = 50 μm.

Fig. 9 In vivo imaging of (A) a mouse untreated (Control); (B) a mouse injected with THPP; (C) a mouse injected with THPP followed injected with Ag^+; (D) a mouse injected with THPP, then injected with Ag^+ followed injected with Cl^-.

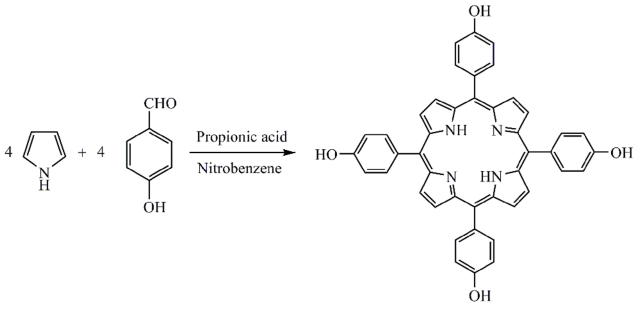

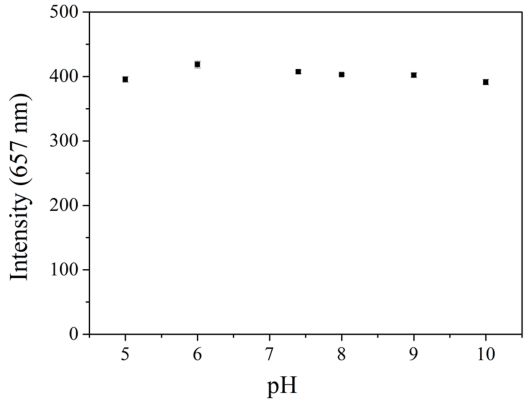

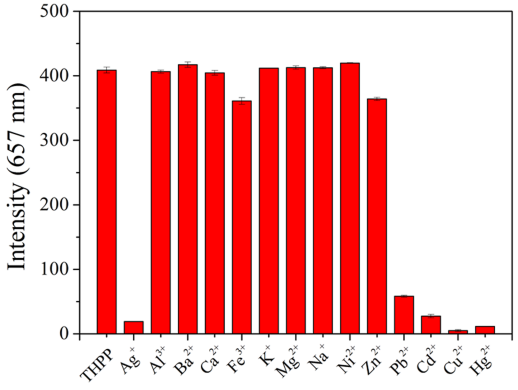

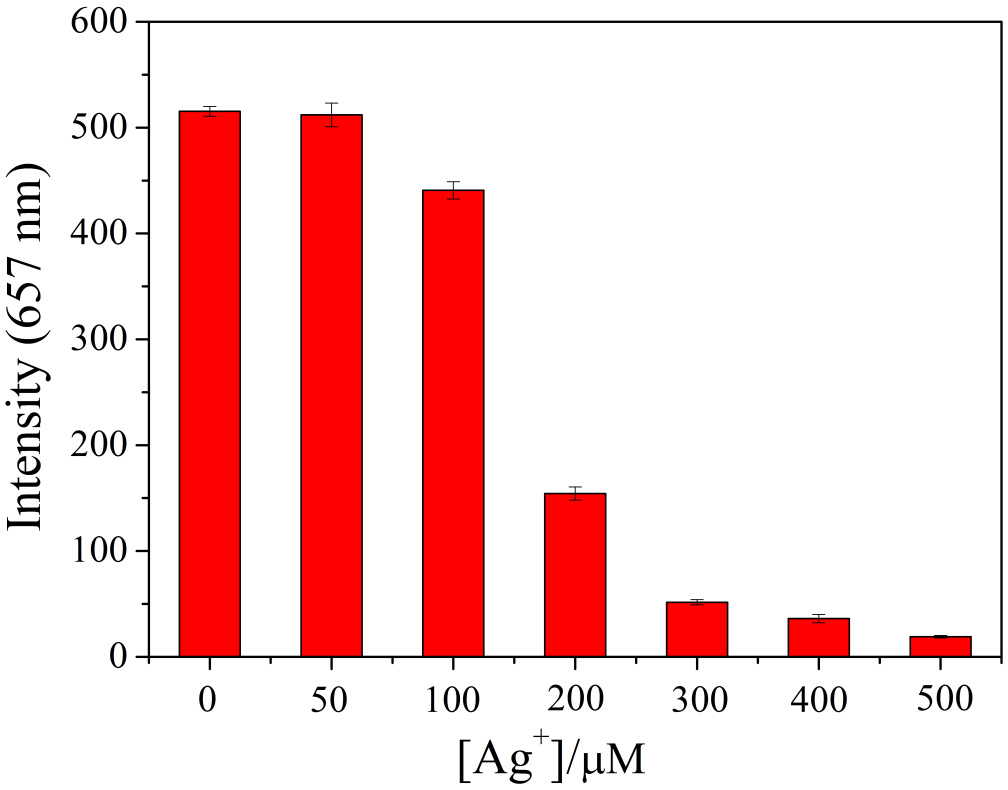
600
500
400
300
200
100
0
Intensity (657 nm)
0
50
100
200
300
400
500
[Ag+]/μM

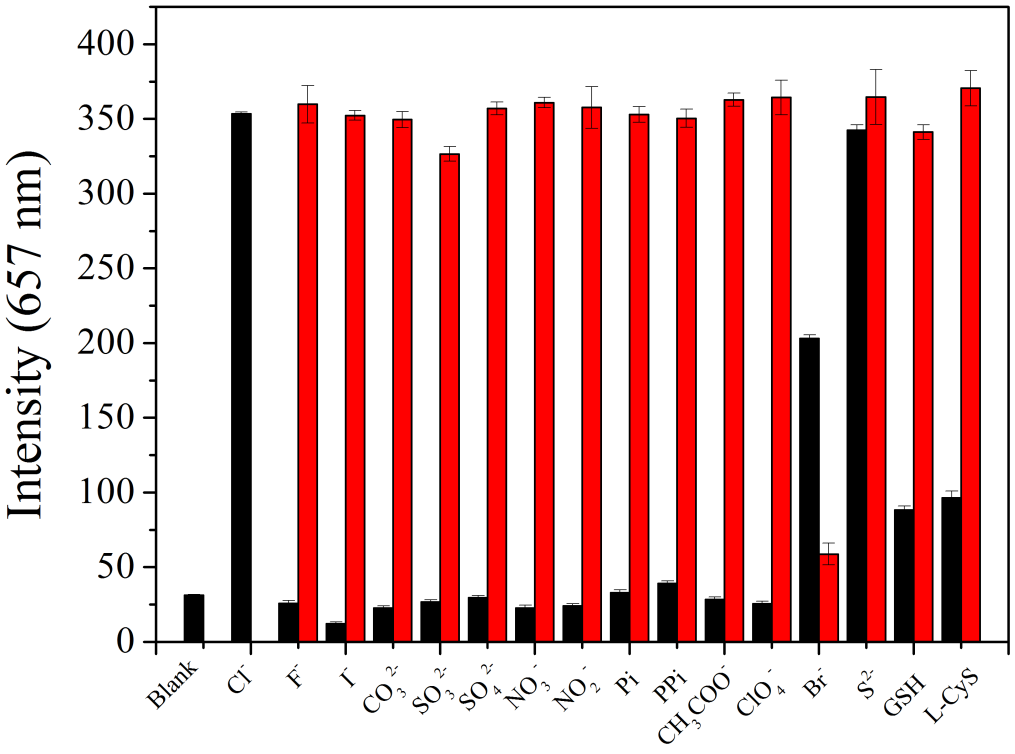
Intensity (657 nm)
400
350
300
250
200
150
100
50
0
Blank
Cl-
F-
I-
CO3 2-
SO3 2-
SO4 2-
NO3-
NO2-
Pi
PPi
CH3COO-
ClO4-
Br-
S2-
GSH
L-CyS

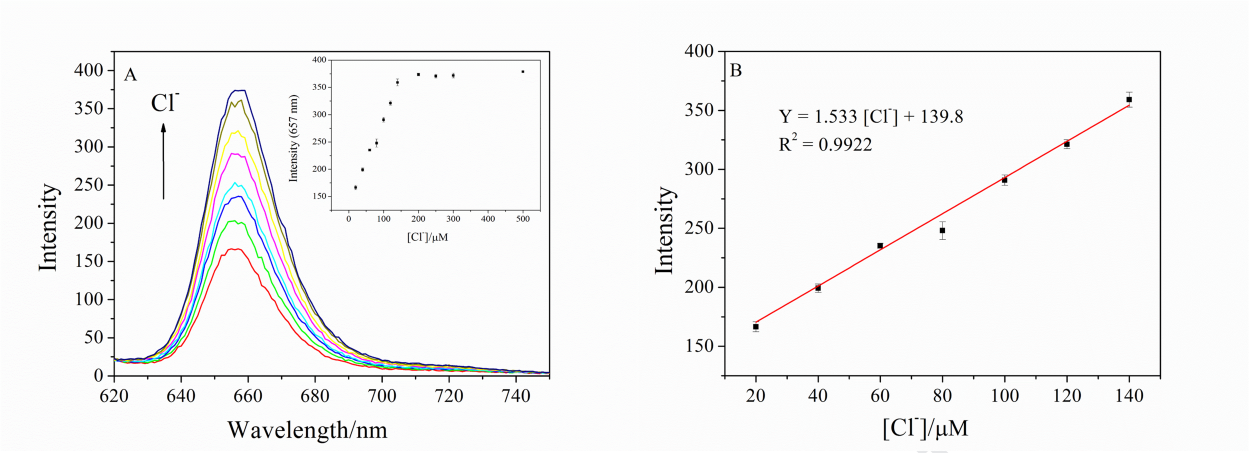

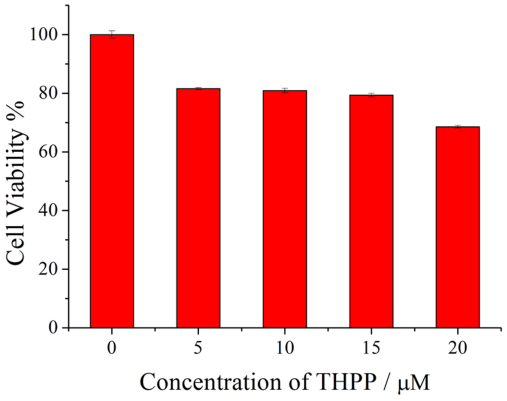

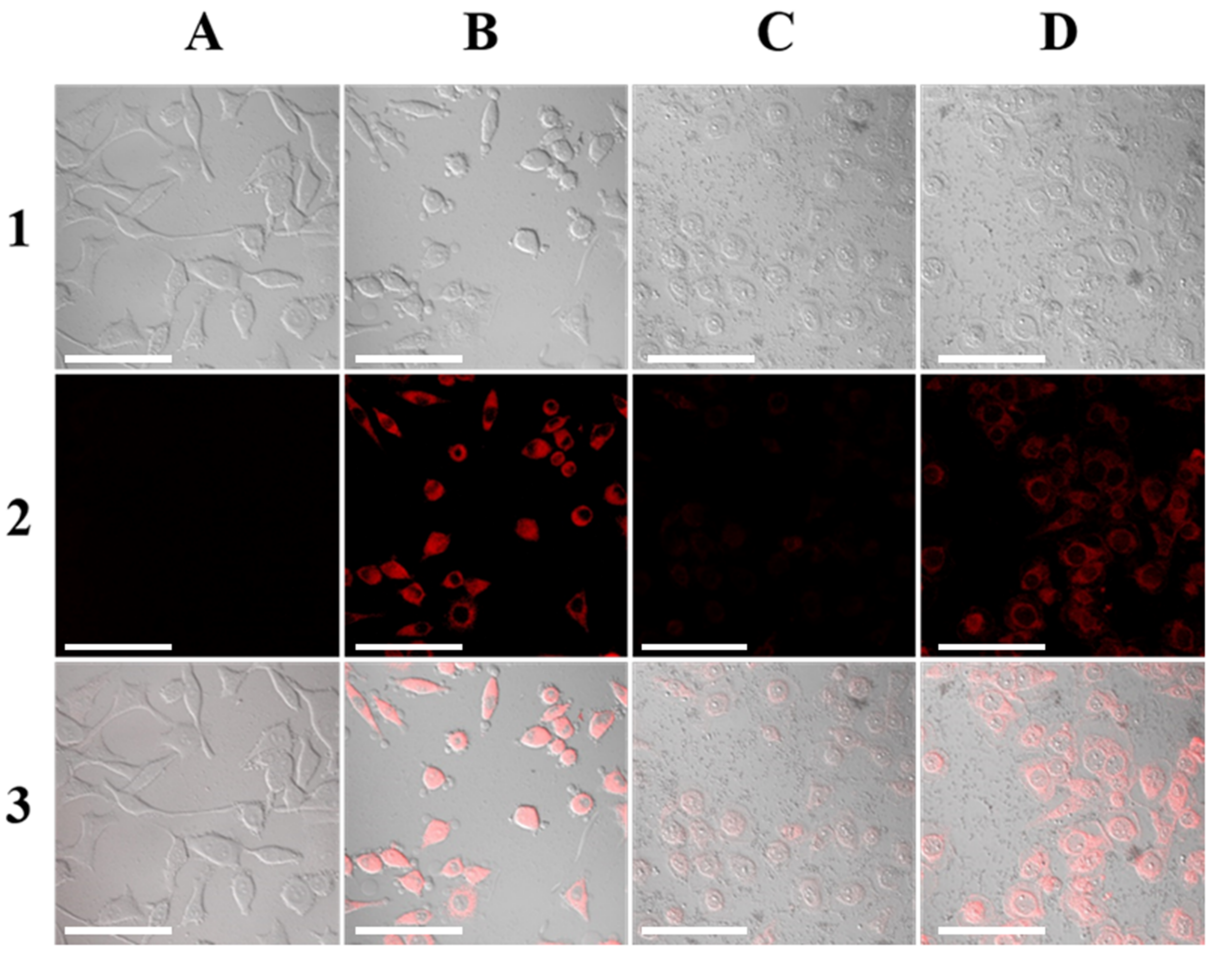

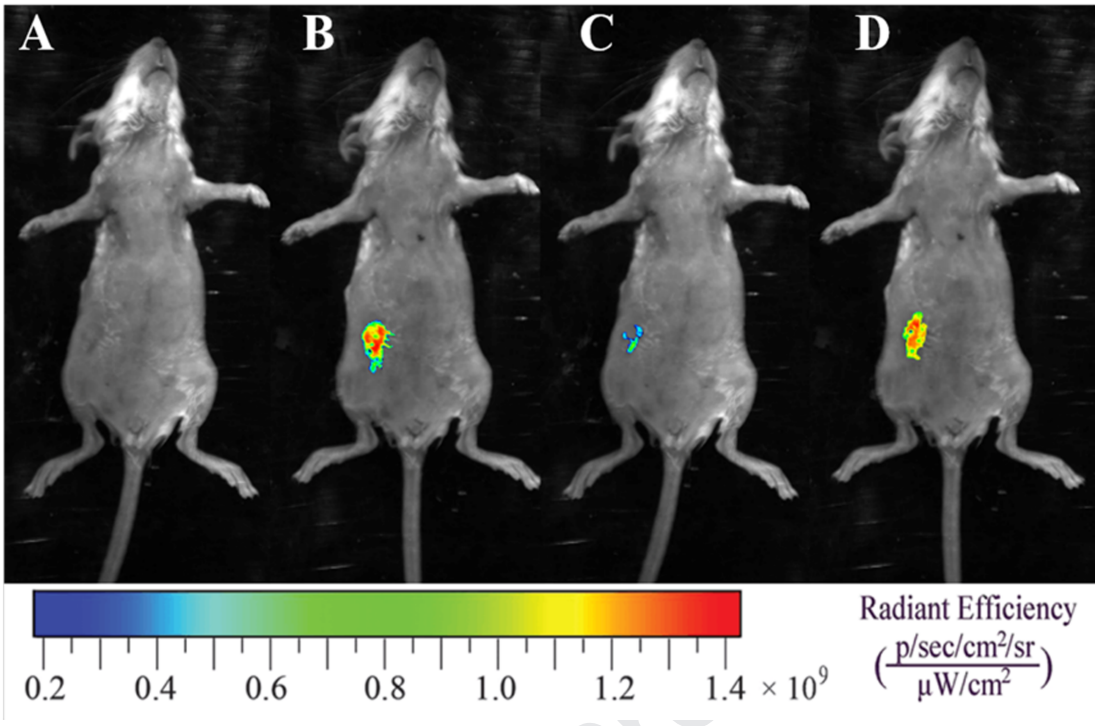

Highlights:

- NIR fluorescence turn-on detection of chloride ions under physiological condition
- The sensor has preferable selectivity and sensitivity compared with reported.
- The sensor can be used in bioimaging in vitro and in vivo.

Declaration of Interest Statement

We enjoy Spectrochimica Acta Part A: Molecular and Biomolecular Spectroscopy very much, and would like to submit the enclosed manuscript entitled **"A NIR Turn-on Fluorescent Sensor For Detection of Chloride Ions in Vitro and in Vivo",** which was to be considered for publication in Spectrochimica Acta Part A: Molecular and Biomolecular Spectroscopy.

No conflict of interest exists in the submission of this manuscript, and manuscript is approved by all authors for the submission. The corresponding author is Dr Haixia Zhang, the co-authors are Fengyuan Zhang, Chen Ma, Zhijuan Jiao, Shuai Mu, Yida Zhang, Xiaoyan Liu. I would like to declare on behalf of my co-authors that the work described was original research that has not been published previously, and not under consideration for publication elsewhere.